Femtosecond Pumping Rate Dependence of Fragmentation Mechanisms in Matrix-Assisted Laser Desorption Ionization

Cornelius L. Pieterse,[†] Frederik Busse,[†] Friedjof Tellkamp,[†] Wesley D. Robertson,[†] and R. J. Dwayne Miller[*,†,‡]

[†]*Max Planck Institute for the Structure and Dynamics of Matter, Luruper Chaussee 149, 22761 Hamburg, Germany*

[‡]*Departments of Chemistry and Physics, University of Toronto, 80 St. George Street, Toronto, Ontario, M5S 3H6, Canada.*

E-mail: dwayne.miller@mpsd.mpg.de

Abstract

The benzyltriphenylphosphonium (BTP) thermometer ion is utilized to characterize the fragmentation mechanisms of matrix-assisted laser desorption/ionization (MALDI) for femtosecond ultraviolet laser pulses. We demonstrate that the survival yield of BTP approaches unity under these conditions, which suggests that a minimal amount of fragmentation is occurring. It is also shown that the survival yield of BTP is insensitive to the laser fluence. However, the magnitude of fragmentation for the matrix increased notably for the same fluence range. These results indicate that the amount of energy transferred from the matrix ions to the BTP thermometer ions is minimal because the femtosecond desorption applied here occur within the stress-confinement regime. This observation is in agreement with recent molecular dynamics simulations which predict that it should be possible to separate both desorption and ionization processes in the regime of stress-confined desorption. Our results indicate that angiotensin is the largest biomolecule which could be routinely measured with these pulses. A mass upper-limit supports the hypothesis that ionization is hindered by the increased thermal gradients imposed in the lattice and associated velocity distribution within the ablation process from the much higher lattice heating rate with femtosecond pulses. This effect results in the temporal overlap between the neutral molecules and the matrix ions being too small to result in sufficient proton exchange for ionization.

Graphical TOC Entry

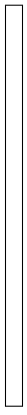

Introduction

Shortly after the initial reports by Karas and Hillenkamp on the analysis of large biomolecules using matrix-assisted laser desorption/ionization (MALDI),[1] the influence of the laser pulse duration on the desorption/ionization mechanism was discussed.[2] This study demonstrated that ultrashort (femtosecond) pulses could be applied similarly to that of nanosecond pulses, with the only recognized disadvantage being that there exists an accessible mass upper-limit. In this study, Demirev *et al.* compared the mass spectra generated by using either a nitrogen ($\lambda = 337$ nm, $\tau = 3$ ns) or a dye laser ($\lambda = 248$ nm, $\tau = 560$ fs) interfaced to a linear time-of-flight mass spectrometer. This was the first study to illustrate that the MALDI process is primarily dependent on laser fluence and not the peak power to a first approximation. It was also observed that the intensity of insulin ions ($\sim$5000 Da), relative to the ferulic acid matrix ions, was significantly smaller for the femtosecond versus nanosecond pulses.[2] Following this study, there have only been a small number of studies investigating ultrashort pulses for the purpose of desorbing and ionizing biomolecules in MALDI.[3–6] In support of this observation, when comparing the photoionized neutrals, and directly desorbed ions, for two nitrogen lasers (550 ps versus 3 ns), Dreisewerd *et al.* reported that the only difference between the spectra produced by these lasers was a small difference in the fluence thresholds.[3] This finding would be consistent with some loss of deposited laser energy out of the irradiated zone during the pulse duration, which does occur by acoustic transport on this timescale. Papantonakis *et al.* performed a comprehensive study in order to help illuminate the ionization mechanisms by comparing the mass spectra produced by a nitrogen ($\lambda = 337$ nm, $\tau = 3$ ns), a Nd:YAG ($\lambda = 266$ nm, $\tau = 2$ ns) and also a Ti:Sapphire ($\lambda = 266$ nm, $\tau = 120$ fs) laser.[4] In agreement with the earlier reports, their mass spectra appeared nearly identical for all of the different systems investigated. However, it should be mentioned that their analytes were diluted to relatively low matrix-to-analyte ratios (100:1 for angiotensin II and β-cyclodextrin and 10:1 for erythromycin), which is in contrast with other investigations where this ratio is generally at least an order of magnitude larger.[2–7] It is well-established that for a matrix-to-analyte ratio smaller than $\sim$100, the matrix peaks are quite often suppressed relative to the analyte peaks, so it is difficult to compare these results with those of other studies.[7,8] Nevertheless, for the majority of their reported mass spectra, the analyte-to-matrix peak ratio was smaller for the femtosecond versus nanosecond pulses.[4]

The first quantitative comparison between ultrashort picosecond ($\lambda = 355$ nm, $\tau = 22$ ps) and nanosecond ($\lambda = 337$ nm, $\tau = 4$ ns) pulses were performed by Chen and Vertes through studying various biomolecules prepared in the matrixes 2,5-dihydroxybenzoic acid (DHB),[9] sinapinic acid (SA), and also α-cyano-4-hydroxycinnamic acid (CHCA) pellets.[5] Their results corroborated all of the previous observations for ultrashort pulses, while also reporting that all of the investigated matrices are significantly more likely to fragment when irradiated with the longer pulses. Most importantly, analogous to the observation for femtosecond pulses,[2] it was reported that insulin was the largest molecule to be detected with picosecond pulses. The explanation was that considering the high optical pumping rates achievable with picosecond

pulses, the temporal overlap within the desorption plume between these neutral biomolecules and the matrix ions is too small to result in sufficient proton exchange for efficient ionization.[5] This higher rate of energy deposition, and ensuing ablation dynamics, lead to higher velocities of the ejected molecules, which has been quantified in a different context by Franjic *et al.*[10] Furthermore, since internal energy of molecular ions determine their accessible fragmentation pathways, a determination of their survival yields is a compelling technique for characterizing the softness of a given desorption method.[11–13] For a similar reason, the collisional transfer of energy from the matrix to the analyte ions was investigated by employing the thermometer ion benzyltriphenylphosphonium (BTP) in a subsequent study.[6] The simple structure and known fragmentation channels of the benzylpyridinium species render them to be attractive candidates to monitor the transfer of energy during the desorption process because they are already present in the solid phase as preformed ions.[14–16] Comparing these nanosecond and picosecond lasers, it was reported that the picosecond pulses resulted in a lower net transfer of energy.[6] This observation was interpreted to be the result of picosecond desorption occurring under stress-confinement conditions, whereas the nanosecond desorption process was only thermally confined.[17] Molecular dynamics simulations suggested that when operating under stress-confinement conditions, both desorption and ionization processes should be separable, which would allow unique control over measurement conditions.[18] This prospect has recently raised interest in the resonant excitation and ablation of both aqueous solutions and tissues using picosecond infrared lasers to facilitate extremely soft material extraction under stress-confinement conditions.[10,18,19] The usage of this method demonstrated that it is possible to extract proteins and enzymes while conserving their quaternary structures.[20,21]

All of the mentioned studies almost exclusively employed laser excitation in the common reflection geometry. The use of the transmission geometry has been reported during the early days of MALDI,[22–25] but it has never attracted a significant amount of interest. However, the highest imaging spatial resolution has been reported recently by using such a geometry, which indicates that there is clearly a need for revisiting the application thereof, since there are less geometrical restrictions with regards to the focusing optics.[26,27] Moreover, the temperature gradient imposed in the sample creates a force which directs the ablated molecules along the analyzer collection axis. The temperature rise is highest at the back surface of a sample and smallest at the front. The corresponding velocity gradient of the excited molecules is along the surface normal. In reflection, the temperature gradient is in the opposite direction and ablation into the ion collection optics requires recoil forces to redirect the ablated molecules. This difference may be small for sufficiently thin samples, but still, a difference to be noted. The qualitatively similar results obtained when comparing the transmission to the reflection geometry for imaging of cells is, however, indicative that sample thickness is not a point at issue.[26] Nevertheless, a quantitative study to determine whether the transmission geometry is inferior to its reflection counter-part would be highly beneficial to future instrumentation developments. Vertes *et al.* were the first to realize the transmission geometry on a modified LAMMA 500-type system.[22] Several peptides were analyzed by applying the solutions to

transmission electron-microscope grids without the presence of a metallic substrate. One of their main conclusions was that since high-quality spectra were obtained, the participation of the metal substrate in the desorption process is, therefore, less likely.[22] Heise and Yeing studied the desorption process dynamics by employing a quartz microbalance, and although no mass spectra were generated, it was shown that the desorption thresholds are higher for the transmission geometry.[23]

Schürenberg *et al.* were the first and only to perform a comparison between the reflection geometry and the transmission geometry for both peptides and proteins, where they noticed distinct differences for the plume dynamics.[24] Similar to earlier studies by these authors,[28] both geometries were investigated using a fibre-coupled nitrogen laser with a relatively large ($\sim$200 μm) spot size. Although both DHB and CHCA generated good quality, qualitatively similar mass spectra, CHCA resulted in less reproducible results, unless special sample preparation methods were employed. Similar to the earlier studies,[23] the threshold fluences tended to be slightly larger for the transmission geometry. A notable result from this study was that the mean ion velocities for the transmission geometry were significantly lower than those of the reflection geometry. The discrepancy was attributed to the spatial confinement within a thick sample layer and the resulting turnaround time it takes for molecules to be accelerated towards the ion extraction optics.[24] However, it should further be pointed out that the finite optical penetration depth (100 nm) and significant differences in surface temperature (facing analyzer input) will too contribute to both the observed higher threshold fluence and velocity distribution.[29] Nevertheless, it was shown that the spectra are still in quantitative agreement for both geometries, especially with regards to mass resolution and analyte fragmentation.[24] With back illumination, or a transmission geometry, it is possible to place lenses much closer to the sample and even use an oil or solid immersion lens to focus below 1 μm readily. Given this potential for an increased spatial resolution for mass spectrometry imaging, we found it surprising that other than the above studies, there has been little adoption of transmission geometries over the standard reflection geometry.

In this work, we report on the use of femtosecond desorption in the transmission geometry by probing the fragmentation mechanism of the well-established BTP thermometer ion. This study provides information on the energy redistribution and transduction to the desorption process and its subsequent effect on the ion yields most relevant to use in mass spectrometry. The survival yield of the BTP is shown to approach unity for the pulse energies studied, which is in agreement with molecular dynamics simulations which anticipated that the desorption and ionization processes would become separable under stress-confinement conditions. We, therefore, demonstrated that a transmission geometry with femtosecond lasers could be used in a similar fashion as to the standard reflection geometry with nanosecond lasers, with the potential for much higher spatial resolution for mass spectrometry imaging.

Experimental

Experiments were carried out on a home-built linear time-of-flight mass spectrometer, which is schematically illustrated in Figure 1. The samples were desorbed using the third harmonic ($\lambda = 343$ nm, $\tau = 190$ fs) output of a regeneratively amplified Yb:KGW oscillator (Pharos SP 1.5mJ, Light Conversion, Vilnius, Lithuania) with an output pulse-to-pulse stability better than 0.5% rms over 24 hours. The measurements were performed in a transmission geometry by focusing the near-Gaussian beam to a spot diameter of 225 ± 7 μm (per $1/e^2$ definition) at the sample surface using a $L = 750$ mm lens (LA4716-UV-ML, Thorlabs GmbH, Munich, Germany) located outside the vacuum chamber. The spot size was regularly determined with high-precision knife-edge measurements. The pulse energy could be set between 2 and 10 μJ, as measured before experiments using a calibrated photodiode (S120VC, Thorlabs GmbH), resulting in peak fluences of between $\sim$100 and 500 J/m^2 at the sample surface. The sample holder was mounted on three nanometer-precision stages (SLC series, SmarAct, Oldenburg, Germany) which enabled an area of approximately 1×1 cm^2 to be scanned relative to the laser focal position. The sample was imaged from the backside using a long working distance microscope (Optem Fusion, Qioptiq Photonics GmbH, Göttingen, Germany). We note here that this geometry can readily be improved for smaller spot diameters at the sample position. The present geometry was easiest to implement with the present sample holder design.

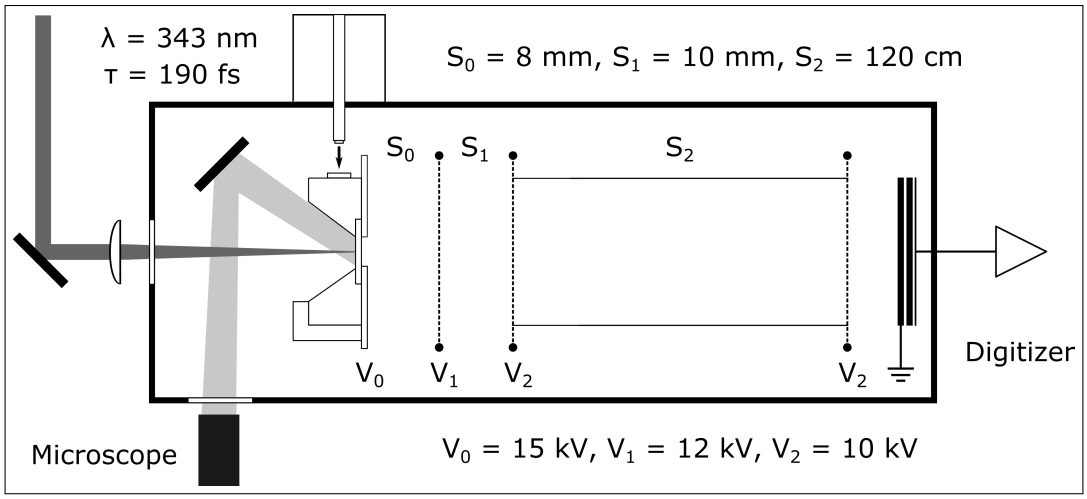

Figure 1: Experiments were performed in a transmission geometry on a linear time-of-flight mass spectrometer, in which the laser beam strikes the backside of the substrate co-linearly with the ion extraction axis. Refer to text for further details (figure not drawn to scale).

Following desorption, positive ions were accelerated to a nominal kinetic energy of 5 keV in a static, two-stage extraction region, supplemented with an 10 keV post-acceleration stage, resulting in a total energy of 15 keV upon reaching the detector.[30] In order to achieve these conditions, the sample and the extraction grid was maintained at 15 and 12 kV, respectively; while the flight tube was maintained at 10 kV to facilitate a post-acceleration. The distances

along beam axis S were fixed to $S_0 = 8$ mm between the sample surface and extraction grids, and to $S_1 = 10$ mm between the extraction grid and the field-free drift region, which had a length of $S_2 = 120$ cm. Stabilized, high-precision, digital power supplies were employed for all of these experiments (EHS series, Iseg Spezialelektronik GmbH, Radeberg, Germany). Only positive ions were measured using a dual-stage chevron microchannel plate detector (F9890, Hamamatsu, Bridgewater, USA) with a built-in signal decoupling circuit, which was recorded using an 8-bit digitizer (DC211, Acquiris, Plan-les-Ouates, Switzerland). Signal acquisition was triggered by a fast photodetector (DET10A/M, Thorlabs) located to measure stray light. Synchronization was coordinated by using a computer controlled delay generator (DG645, Stanford Research Systems, Sunnyvale, USA). The pressure inside the mass analyzer region was generally better than 2.0×10^{-7} mbar immediately after sample loading, improving to a pressure of better than 8.0×10^{-8} mbar at the end of the measurements.

Double side polished fused silica wafers of $\sim$1 mm thickness were employed as the sample substrate, which is transparent in the wavelength range studied. The surface of a single side was roughened with 600 grit sandpaper, facilitating small crystal formation and therefore improving sample homogeneity. Substrates were cleaned according to established MALDI protocols, stored in ethanol, and finally, air dried with a nitrogen gas stream before usage.[31] The analytes, benzyltriphenylphosphonium chloride (99 %) and angiotensin I acetate salt hydrate (90 %), were purchased from Sigma-Aldrich Chemie GmbH (Munich, Germany). The matrix DHB was purchased from Bruker Daltonik GmbH (Bremen, Germany). Analyte solutions (0.1 mg/ml) were prepared in deionized water (PURELAB Classics, ELGA) with 0.1% trifluoroacetic acid (TFA). The matrix solution (10 mg/ml) was prepared in a standard 1:2 (v/v) mixture of acetonitrile and deionized water with 0.1% TFA.[32] All chemicals were used without further purification.

Matrix and analyte solutions were mixed 1:2 to yield a molar matrix-to-analyte ratio of $\sim$3000.[5,13] Droplets containing 3.0 μl of this mixture were spotted on the roughened substrate and rapidly vacuum dried to produce more uniform crystals,[13,33] since this protocol is known to result in improved quantification and reproducibility.[34,35] In addition, for all of the results presented here, the samples were prepared in a single spotting and drying cycle to ensure that the crystallization conditions were identical, and only those samples showing similar dried droplet sizes were selected. The results obtained with the matrix CHCA was of an inferior quality compared to the DHB and the repeatability was challenging (other workers have also made this observation, especially for a transmission geometry).[24,34] Because of these reasons, it was decided to focus on DHB in this study exclusively. The laser spot size, fluence, sample preparation protocol, and the magnitude of the extraction and post-acceleration fields was implemented in accordance with the conditions previously employed for the transmission geometry to facilitate a quantitative and reproducible comparison.[24,28]

The lowest fluence reported here (126 J/m^2) was about 1.5 times greater than the DHB matrix fragmentation threshold and was selected because BTP did not significantly fragment for the studied fluence range. Usage of the matrix fragmentation threshold was motivated by observing that the fragmentation thresholds of the DHB matrix[5] and BTP thermometer[6] ions were comparable for picosecond pulse durations.[5,6] The complete area associated with a given sample was scanned for laser fluence values within a range between 1.5 and 2.7 times the fragmentation threshold. Only those single shot spectra for which the largest peak was above a defined threshold were averaged while each spectrum was calibrated using the DHB matrix and BTP thermometer parent ion peaks. This strategy resulted in about 500 spectra being averaged per sample, with the resulting spectrum, therefore, being more representative of a sample, in contrast to measuring a large number of spectra at a single position.

Following the same methodology as previous studies,[6,13] survival yields α were calculated as $\alpha = \sum I_M / \left(\sum I_M + \sum I_F\right)$, where $\sum I_M$ and $\sum I_F$ are the integrated absolute abundances of the quasi-molecular parent and fragment ions respectively.[16] The dehydroxylated fragment was considered for DHB, while for BTP both the benzyl and triphenylphosphine fragments were considered. The resulting yield distribution was then examined to determine the mean survival yields. Following such an approach assumes that all of these ions have both identical collection and detection efficiencies, which is a reasonable assumption for the small molecules investigated in this work. However, should molecules larger than approximately 1000 Da be studied, then it would be required to account for mass-limited detector efficiencies.[36,37]

Results and discussion

Following the same methodology as previous studies, which compared the effects of different pumping rates on the MALDI mechanism,[5,6] the survival yields for both the DHB matrix[5] and the BTP thermometer[6] ions were measured for various fluences. A typical mass spectrum obtained for studying such a fragmentation mechanism is shown in Figure 2, from which the DHB matrix (m/z=154) and BTP thermometer (m/z=353) parent ion peaks are visible. It is immediately clear that the BTP only slightly fragmented since the peaks associated with both the benzyl (m/z=91, fragment F1) and triphenylphosphine radicals (m/z=262, fragment F2) are hardly visible. However, the dehydroxylated DHB ion (m/z=137) is pronounced.

Figure 3 shows the peaks of interest normalized to the DHB and BTP parent ion peaks for different fluences. Unfortunately, similar crystallization conditions could only be achieved for a limited number of samples within one batch, limiting the number of fluence data points. Nevertheless, the reproducibility between samples within the same batch was sound, such as shown in Figure S1 for several measurements performed under similar conditions. The mean survival yields for DHB and BTP, as averaged over the complete sample area, are shown in Figure 4. Within experimental uncertainty, the BTP survival yield ($\sim$0.95) was independent of the fluence for the energies studied (1.5 to 2.7 times the matrix fragmentation threshold).

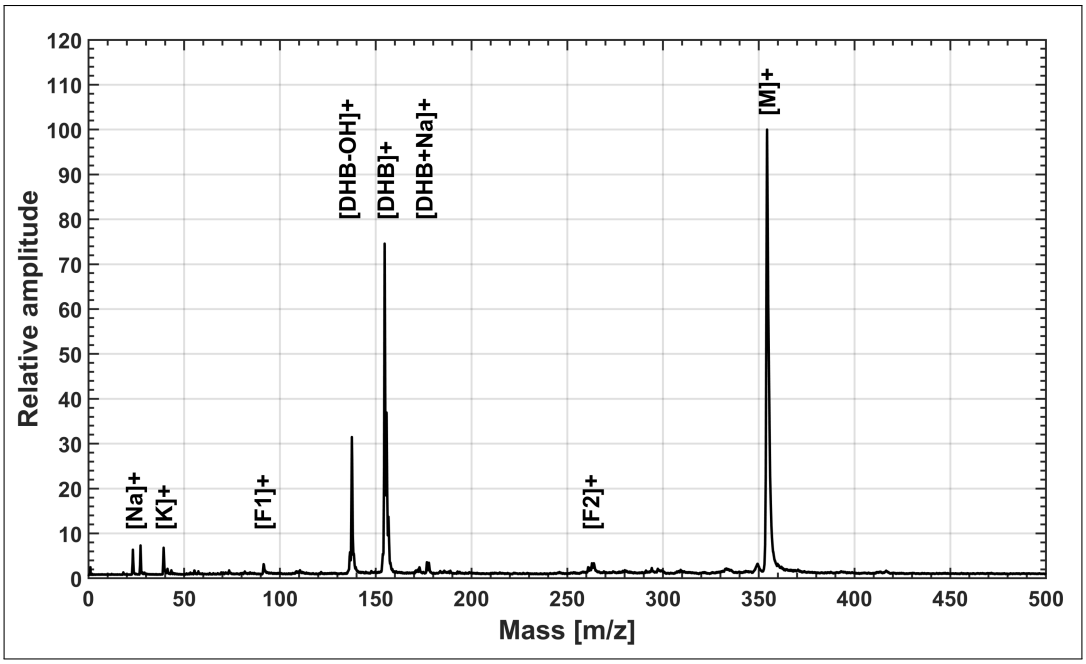

Figure 2: Mass spectrum for the low fluence (126 J/m^2) measurement showing the molecular BTP thermometer ion (m/z=353) and the DHB matrix ion (m/z=154), as well as both the BTP thermometer ion fragments. Refer to the text for additional details.

The shot-to-shot and position dependent signal fluctuations are characterized by the survival yield histogram shown in Figure 4. This histogram shows the survival yield of the BTP ions for the lowest fluence measurement, which exhibits the same characteristic features as noted from previous studies.[13] Since this distribution is skewed, the maximum survival yield is in reality much higher than the given mean. These results indicate that the DHB fragmentation threshold is lower than that of BTP and that even under conditions where large portions of the DHB fragment, the BTP still remains intact. Nevertheless, these survival yields are still suitable to monitor the energy content of the ions and the associated transfer thereof. Since these measurements were performed under conditions where the Keldysh parameter is in the excess of 50, multiphoton ionization will be the prevailing ionization mechanism.[38–40]

In comparison, the previous study with 22 ps pulses reported a lower BTP survival yield ($\sim$0.87) which was notably more sensitive to the fluence.[6] While the results presented there contained a large uncertainty, they showed a distinct decrease in BTP survival yield ($\sim$0.67) when increasing the fluence to 1.3 times the BTP fragmentation threshold. Moreover, even lower survival yields were observed for nanosecond pulses.[6] Even though care should be taken when comparing these different threshold definitions, we believe we observed a continuation of the trends reported for that comparison of nanosecond and picosecond pulse durations: a higher survival yield for the shorter pulse durations.[6] The reduced transfer of energy from the matrix to the analyte molecules can be explained by the high-pressure gradients which result from a stress-confined desorption; the energy deposition step is completed well before

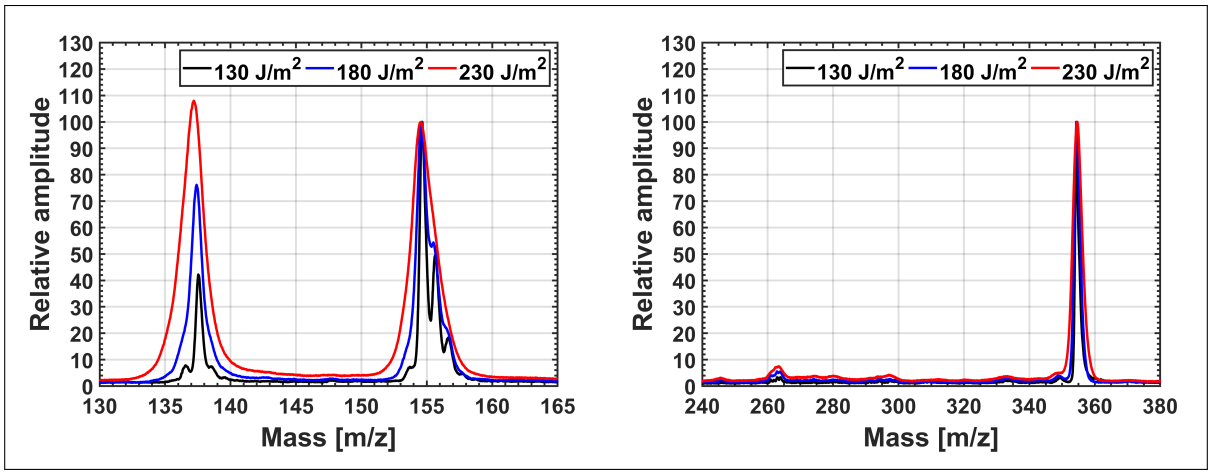

Figure 3: Mass spectra of the DHB matrix (left) and BTP thermometer ions (right) for the fluences studied. Spectra was normalized relative to the parent peaks only for presentation. The survival yields were calculated using the absolute signal intensities.

any noticeable movement of the sample material can occur,[17] which results in a very small amount of time during which species can interact.[5] The picosecond pulses only resulted in a partial stress-confinement,[6] while the femtosecond pulses used here lead to a fully stress-confined desorption and transferred even less of the deposited energy from the lattice to the thermometer ions, as inferred from the minimal fragmentation. Although spectral variations in the absorption coefficient could potentially yield an alternative explanation of the observed trend, recent results indicate the differences in wavelength between the different lasers would not explain the different survival yields.[41,42]

It should be noted that a lower matrix fragmentation threshold (84 J/m^2) was observed than for previous studies. However, since the present spot size (225 μm) is considerably larger than for the picosecond studies (55 μm), the different fragmentation thresholds should not be unexpected: earlier studies have shown that thresholds are a function of the spot size.[43–45] It is established that by using the threshold fluence of the small spot size for a larger spot size would result in both extensive fragmentation and loss of mass resolution.[28,45] The reasons for this, with either linear or nonlinear absorption, is that ablation physics under the same conditions should be the same. The difference may have to do with the scales of the thermal gradients or in-plane stress forces relative to the crystal grain sizes that leads to the spot size dependence. We note that the detection threshold of DHB for the spot size of this study is in accord with previous studies.[28,42] For a better comparison, we will only compare the relative increase of the pulse energy above the fragmentation threshold, since that will determine the relative magnitude of fragmentation. Notice that the micron sample thickness is considerably thicker than the penetration depth, which suggests that these ions most probably originated from the back surface of the sample.[24]

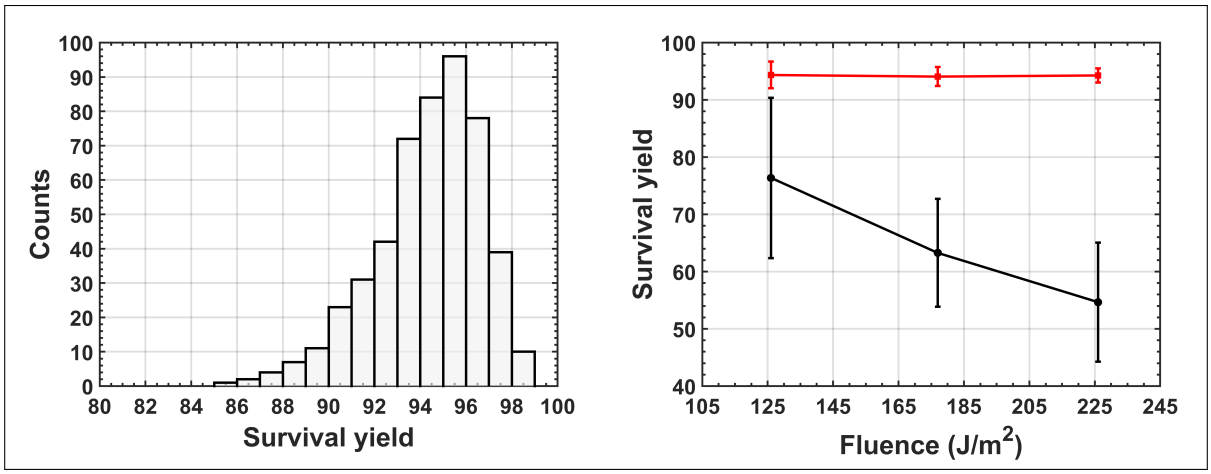

Figure 4: Survival yield distribution (left) of the BTP thermometer ions for the low fluence (126 J/m^2) measurements involving ∼500 independent measurements. Mean survival yields (right) of the BTP (red) and DHB (black) ions are shown for the fluence range studied.

It is important to highlight that fragmentation of the DHB matrix increased significantly for the maximum pulse energies studied. Earlier pumping rate studies did not consider a very broad fluence range for the ultrashort pulses, which impedes detailed comparisons from being performed. Most importantly, the previous studies only reported either on the DHB matrix[5] or the BTP thermometer[6] ions, but a combined analysis was unfortunately not performed. However, these studies did indicate that the fragmentation thresholds of the DHB and BTP ions were comparable for the picosecond pulse durations. A similar observation has also been made when studying liable biomolecules using nanosecond pulses.[46] Assuming unimolecular reactions, the internal energy becomes equivalent to the concept of an effective temperature. It is established that the effective temperature within the desorption plume can be deduced from the extent of matrix fragmentation.[47,48] Therefore, considering earlier studies, combined with both the peak broadening and excessive matrix fragmentation observed for high fluence values,[43] it is clear that these measurements were performed under unusually hot conditions. The following step would be to investigate these dynamics by using delayed extraction since it has been shown that the survival yield tends to be higher under such conditions.[14,15]

These observations, therefore, provide further support for the hypothesis that the amount of internal energy transferred from the DHB matrix ions to the BTP thermometer ions were minimal, even though a considerable amount of material has been ejected into the gas-phase. Molecular dynamics simulations describing the desorption of a model peptide by a picosecond infrared laser anticipated a similar observation: when operating under the conditions of stress confinement, the desorption and ionization processes should be separable, therefore allowing the desorption process to be optimized by adjusting the pulse fluence, followed by optimizing the ion separation process by using an appropriate electric field.[18]

In order to understand the fragmentation mechanism inherent to the desorption process, it is required to experimentally isolate this process while also mitigating other fragmentation mechanisms. Another common fragmentation mechanism is meta-stable decay, which occurs along the drift tube as a consequence of the collisional energy acquired by ions from multiple collisions with neutral molecules within the desorption plume.[49–52] The prevailing approach is to reduce the transfer of collisional energy by implementing delayed extraction.[52] As a result of this approach, it is thus possible to probe certain temporal characteristics that is associated with the desorption process.[14] However, due to the added level of complexity, experiments are often instead performed under continuous conditions. The usage of post-acceleration[51] make it possible to employ a lower extraction field within the source region, which will reduce the ion collisions, but still ensures that the ions have sufficient kinetic energies to result in unity detection efficiencies.[36] The main disadvantage of this approach is that the time window for metastable decay to occur is increased,[49] but since measurements were performed under low residual gas pressures, the probability of this occurring was significantly reduced.[52] Another advantage of the post-acceleration scheme is that the fragments formed within the drift tube will also be accelerated to sufficient kinetic energies for detection.[51] Even though it was not within the scope of the present study, a preliminary analysis shows that the magnitude of the metastable fragmentation occurring is minimal. Given that static extraction conditions were used, it was unexpected that only such a small amount of meta-stable decay occurred.[53] To rule out the low extraction field conditions, measurements were performed under considerably higher extraction fields, but there was no significant difference in the results.

The aspect which intrigued us most was the observation that there is a mass upper-limit present when using ultrashort laser pulses for desorption.[2,5] Due to the high-complexity of these measurements, we will only report our qualitative results here. As already mentioned, Demirev *et al.* reported that for their femtosecond pulses (560 fs) a significantly larger yield of the matrix ions was observed.[2] These results were corroborated by a subsequent investigation by Chen and Vertes for picosecond pulses.[5] Our preliminary results supplement both of these observations: angiotensin I ($\sim$1300 Da) was the largest biomolecule which could be routinely measured, even though the intensity thereof was approximately two orders of magnitude less than that of the DHB matrix. However, the possibility remains that this reduction in signal intensity was the consequence of the decreased quantum detection efficiency ($\sim$0.78) because of the mass of this biomolecule.[37] To completely eliminate this possibility, the appropriate detector correction factors have been applied (see Figure S2 for a comparisons). Nevertheless, the overall intensity did not increase significantly. It should also be mentioned that increasing the fluence resulted in a deterioration of mass resolution, but the ratio of analyte-to-matrix ions did not increase. The relative intensity of the peptide did, however, increase upon the usage of delayed extraction, which suggests that the ionization yield was probably increased as more time is available for gas-phase reactions to occur.[51,54] Such an interpretation is in agreement with the hypothesis that due to the very high thermal heating rates of the matrix achievable with ultrashort pulses, the temporal overlap between the net neutral biomolecules

and the matrix ions within the plume is too small to result in sufficient proton exchange for ionization.[5] The molecules are ejected with much higher initial velocities under these ultrafast heating conditions and the different masses would rapidly separate from the increased velocity distribution. There is no time for thermal transport to reduce the thermal gradients prior to the onset of the ablation process, resulting in a much higher initial velocity distribution than with longer pulses (see Franjec *et al.* for the expected plume velocity).[10] Such a mechanism would explain why Chen and Vertes could effortlessly measure insulin molecules using 22 ps pulses, in comparison to our experiments, where we were limited to angiotensin.

Conclusions

We have demonstrated that the survival yields of the BTP thermometer ion approach unity upon desorption with ultraviolet femtosecond pulses. It is shown that, within experimental uncertainty, the fragmentation as a direct consequence of the desorption process is relatively insensitive to the laser pulse energies in the region close to the detection threshold. However, the magnitude of matrix fragmentation into dehydroxylated ions increased significantly over the same pulse energy range. Therefore, combined with the peak broadening observed for the higher pulse energies, it is evident that these measurements were performed under unusually high lattice heating rates, and very fast ablation conditions, which supports the hypothesis that the energy transferred from the matrix ions to the thermometer ions were minimal, in comparison to the plume expansion and adiabatic cooling, even though ample material was ejected into the gas-phase. This observation is in agreement with recent molecular dynamics simulations since those results anticipated that it should be possible to separate desorption and ionization processes using stress-confinement conditions.

We, therefore, observed an extension of an earlier trend identified comparing nanosecond to picosecond pulse durations, which reported a higher survival yield for the shorter pulses. The femtosecond pulses applied here fall within the stress-confinement regime, which would explain why these pulses would transfer less energy form the initially rapidly heated matrix to the thermometer ions than 22 picosecond pulses, which will only lead to a partial stress-confinement. Preliminary results indicated that angiotensin is the largest biomolecule which could be routinely measured. It should be emphasized that the intensity of this peptide was about two orders of magnitude less than that of the matrix. This result supports an earlier hypothesis that the ionization yield is low due the increased velocity dispersion from such rapid ablation conditions and subsequent temporal overlap between the neutral biomolecules and matrix ions being too small to result in sufficient proton exchange for ionization.

Acknowledgement

We would like to thank Djordje Gitaric and Josef Gonschior for their design contributions, as well as Arwen R. Pearson (Hamburg Centre for Ultrafast Imaging, Hamburg, Germany) and Kenneth Robinson (National Centre of Excellence in Mass Spectrometry Imaging, National Physical Laboratory, Teddington, United Kingdom) for valuable comments and suggestions. We are grateful to Susanne Meier for preparing some of the samples. This work was supported by the Max Planck Institute. R. J. Dwayne Miller is the author of a patent (US8110794B2) related to the mechanism of picosecond infrared laser ablation.

Supporting Information Available

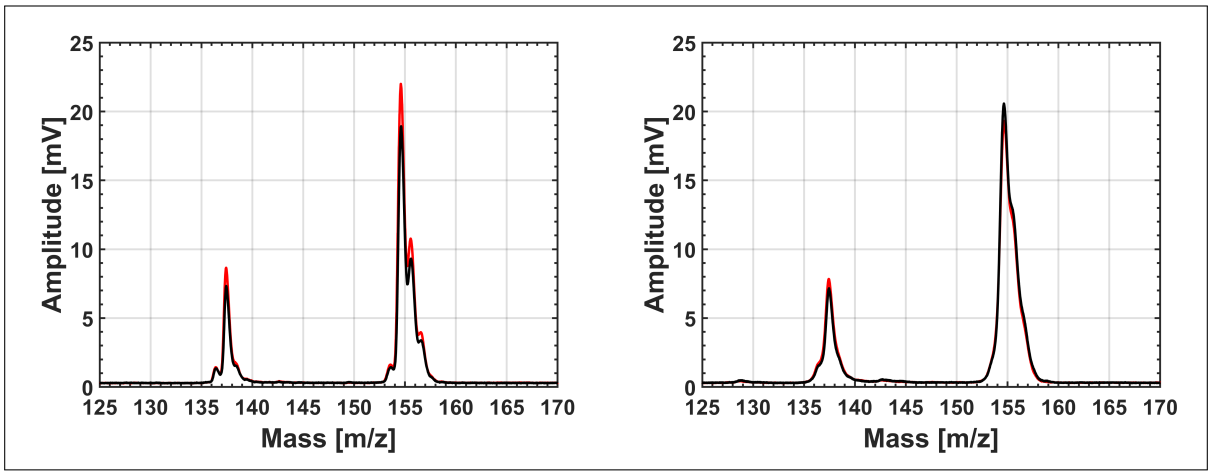

Figure S1: Repeatability is high within a particular batch of samples, such as shown here for measurements performed under identical mass analyzer conditions for two different sample batches. It should be emphasized that identical mass analyzer conditions could be employed with different sample preparation conditions. As an example, comparing these two frames, different matrix-to-analyte ratios were used, which is noticeable from the mass resolution.

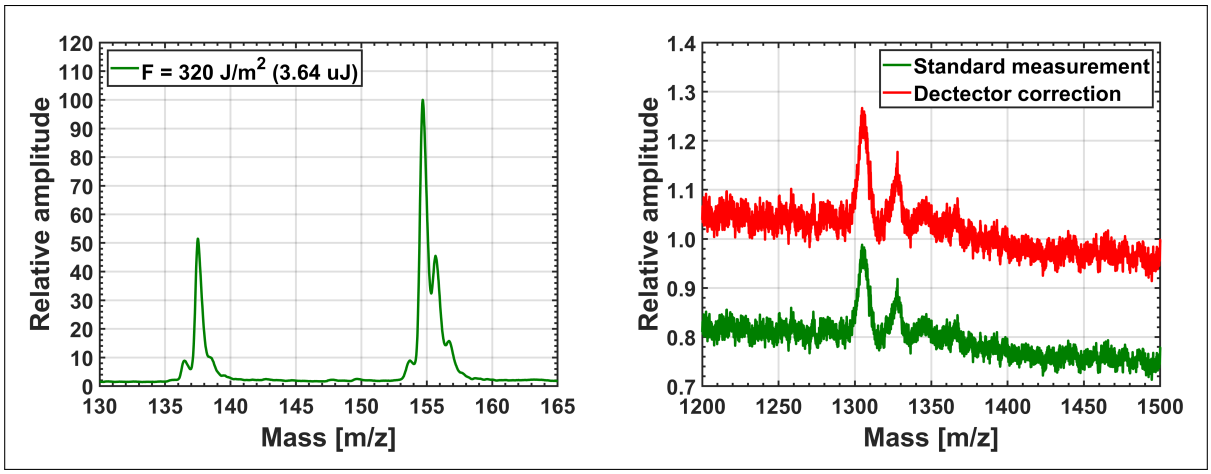

Figure S2: Angiotensin was the largest biomolecule to be routinely measured. Note that the peak intensity thereof was about two orders of magnitude less than that of the DHB matrix. Application of the detector correction factors do not significantly increase the intensity.

References

(1) Karas, M.; Hillenkamp, F. Laser desorption ionization of proteins with molecular masses exceeding 10,000 daltons. *Analytical Chemistry* **1988**, *60*, 2299–2301.

(2) Demirev, P.; Westman, A.; Reimann, C. T.; Håkansson, P.; Barofsky, D.; Sundqvist, B. U. R.; Cheng, Y. D.; Seibt, W.; Siegbahn, K. Matrix-assisted laser desorption with ultra-short laser pulses. *Rapid Communications in Mass Spectrometry* **1992**, *6*, 187–191.

(3) Dreisewerd, K.; Schürenberg, M.; Karas, M.; Hillenkamp, F. Matrix-assisted laser desorption/ionization with nitrogen lasers of different pulse widths. *International Journal of Mass Spectrometry and Ion Processes* **1996**, *154*, 171–178.

(4) Papantonakis, M. R.; Kim, J.; Hess, W. P.; Haglund, R. F. What do matrix-assisted laser desorption/ionization mass spectra reveal about ionization mechanisms? *Journal of Mass Spectrometry* **2002**, *37*, 639–647.

(5) Chen, Y.; Vertes, A. Pumping Rate and Surface Morphology Dependence of Ionization Processes in Matrix-Assisted Laser Desorption Ionization. *The Journal of Physical Chemistry A* **2003**, *107*, 9754–9761.

(6) Luo, G.; Marginean, I.; Ye, L.; Vertes, A. Competing Ion Decomposition Channels in Matrix-Assisted Laser Desorption Ionization. *The Journal of Physical Chemistry B* **2008**, *112*, 6952–6956.

(7) Knochenmuss, R.; Dubois, F.; Dale, M. J.; Zenobi, R. The Matrix Suppression Effect and Ionization Mechanisms in Matrix-assisted Laser Desorption/Ionization. *Rapid Communications in Mass Spectrometry* **1996**, *10*, 871–877.

(8) Knochenmuss, R. The Coupled Chemical and Physical Dynamics Model of MALDI. *Annual Review of Analytical Chemistry* **2016**, *9*, 365–385.

(9) Strupat, K.; Karas, M.; Hillenkamp, F. 2,5-Dihydroxybenzoic acid: a new matrix for laser desorption–ionization mass spectrometry. *International Journal of Mass Spectrometry and Ion Processes* **1991**, *111*, 89–102.

(10) Franjic, K.; Miller, R. J. D. Vibrationally excited ultrafast thermodynamic phase transitions at the water/air interface. *Physical Chemistry Chemical Physics* **2010**, *12*, 5225–5239.

(11) McCrery, D. A.; Peake, D. A.; Gross, M. L. Fast atom bombardment and laser desorption mass spectrometry for determination of alkyltriphenylphosphonium salts. *Analytical Chemistry* **1985**, *57*, 1181–1186.

(12) Claereboudt, J.; Claeys, M.; Geise, H.; Gijbels, R.; Vertes, A. Laser microprobe mass spectrometry of quaternary phosphonium salts: Direct versus matrix-assisted laser desorption. *Journal of the American Society for Mass Spectrometry* **1993**, *4*, 798–812.

(13) Luo, G.; Marginean, I.; Vertes, A. Internal Energy of Ions Generated by Matrix-Assisted Laser Desorption/Ionization. *Analytical Chemistry* **2002**, *74*, 6185–6190.

(14) Gabelica, V.; Schulz, E.; Karas, M. Internal energy build-up in matrix-assisted laser desorption/ionization. *Journal of Mass Spectrometry* **2004**, *39*, 579–593.

(15) Yoon, S. H.; Moon, J. H.; Kim, M. S. A Comparative Study of In- and Post-Source Decays of Peptide and Preformed Ions in Matrix-Assisted Laser Desorption Ionization Time-of-Flight Mass Spectrometry: Effective Temperature and Matrix Effect. *Journal of the American Society for Mass Spectrometry* **2010**, *21*, 1876–1883.

(16) Milasinovic, S.; Cui, Y.; Gordon, R. J.; Hanley, L. Internal Energy of Thermometer Ions Formed by Femtosecond Laser Desorption: Implications for Mass Spectrometric Imaging. *The Journal of Physical Chemistry C* **2014**, *118*, 28938–28947.

(17) Zhigilei, L. V.; Garrison, B. J. Microscopic mechanisms of laser ablation of organic solids in the thermal and stress confinement irradiation regimes. *Journal of Applied Physics* **2000**, *88*, 1281–1298.

(18) Zou, J.; Wu, C.; Robertson, W. D.; Zhigilei, L. V.; Miller, R. J. D. Molecular dynamics investigation of desorption and ion separation following picosecond infrared laser (PIRL) ablation of an ionic aqueous protein solution. *The Journal of Chemical Physics* **2016**, *145*, 204202.

(19) Vogel, A.; Venugopalan, V. Mechanisms of pulsed laser ablation of biological tissues. *Chemical Reviews* **2003**, *103*, 577–644.

(20) Ren, L.; Robertson, W. D.; Reimer, R.; Heinze, C.; Schneider, C.; Eggert, D.; Truschow, P.; Hansen, N.-O.; Kroetz, P.; Zou, J. et al. Towards instantaneous cellular level bio diagnosis: laser extraction and imaging of biological entities with conserved integrity and activity. *Nanotechnology* **2015**, *26*, 284001.

(21) Kwiatkowski, M.; Wurlitzer, M.; Omidi, M.; Ren, L.; Kruber, S.; Nimer, R.; Robertson, W. D.; Horst, A.; Miller, R. J. D.; Schlüter, H. Ultrafast Extraction of Proteins from Tissues Using Desorption by Impulsive Vibrational Excitation. *Angewandte Chemie International Edition* **2015**, *54*, 285–288.

(22) Vertes, A.; Balazs, L.; Gijbels, R. Matrix-assisted laser desorption of peptides in transmission geometry. *Rapid Communications in Mass Spectrometry* **1990**, *4*, 263–266.

(23) Heise, T. W.; Yeung, E. S. Dynamics of matrix-assisted laser desorption as revealed by the associated acoustic signal. *Analytica Chimica Acta* **1995**, *299*, 377–385.

(24) Schürenberg, M.; Schulz, T.; Dreisewerd, K.; Hillenkamp, F. Matrix-assisted Laser Desorption/Ionization in Transmission Geometry: Instrumental Implementation and Mechanistic Implications. *Rapid Communications in Mass Spectrometry* **1996**, *10*, 1873–1880.

(25) Lennon, J. D.; Glish, G. L. A MALDI Probe for Mass Spectrometers. *Analytical Chemistry* **1997**, *69*, 2525–2529.

(26) Zavalin, A.; Todd, E. M.; Rawhouser, P. D.; Yang, J.; Norris, J. L.; Caprioli, R. M. Direct imaging of single cells and tissue at sub-cellular spatial resolution using transmission geometry MALDI MS. *Journal of Mass Spectrometry* **2012**, *47*, 1473–1481.

(27) Zavalin, A.; Yang, J.; Hayden, K.; Vestal, M.; Caprioli, R. M. Tissue protein imaging at 1 μm laser spot diameter for high spatial resolution and high imaging speed using transmission geometry MALDI TOF MS. *Analytical and Bioanalytical Chemistry* **2015**, *407*, 2337–2342.

(28) Dreisewerd, K.; Schürenberg, M.; Karas, M.; Hillenkamp, F. Influence of the laser intensity and spot size on the desorption of molecules and ions in matrix-assisted laser desorption/ionization with a uniform beam profile. *International Journal of Mass Spectrometry and Ion Processes* **1995**, *141*, 127–148.

(29) Lu, I.-C.; Lee, C.; Lee, Y.-T.; Ni, C.-K. Ionization Mechanism of Matrix-Assisted Laser Desorption/Ionization. *Annual Review of Analytical Chemistry* **2015**, *8*, 21–39.

(30) Wiley, W. C.; McLaren, I. H. Time-of-Flight Mass Spectrometer with Improved Resolution. *Review of Scientific Instruments* **1955**, *26*, 1150–1157.

(31) Shen, Z.; Thomas, J. J.; Averbuj, C.; Broo, K. M.; Engelhard, M.; Crowell, J. E.; Finn, M. G.; Siuzdak, G. Porous Silicon as a Versatile Platform for Laser Desorption/Ionization Mass Spectrometry. *Analytical Chemistry* **2001**, *73*, 612–619.

(32) Vorm, O.; Roepstorff, P.; Mann, M. Improved Resolution and Very High Sensitivity in MALDI TOF of Matrix Surfaces Made by Fast Evaporation. *Analytical Chemistry* **1994**, *66*, 3281–3287.

(33) Cohen, S. L.; Chait, B. T. Influence of Matrix Solution Conditions on the MALDI-MS Analysis of Peptides and Proteins. *Analytical Chemistry* **1996**, *68*, 31–37.

(34) Nicola, A. J.; Gusev, A. I.; Proctor, A.; Jackson, E. K.; Hercules, D. M. Application of the fast-evaporation sample preparation method for improving quantification of angiotensin II by matrix-assisted laser desorption/ionization. *Rapid Communications in Mass Spectrometry* **1995**, *9*, 1164–1171.

(35) Gusev, A. I.; Wilkinson, W. R.; Proctor, A.; Hercules, D. M. Improvement of signal reproducibility and matrix/comatrix effects in MALDI analysis. *Analytical Chemistry* **1995**, *67*, 1034–1041.

(36) Gilmore, I.; Seah, M. Ion detection efficiency in SIMS:. *International Journal of Mass Spectrometry* **2000**, *202*, 217–229.

(37) Liu, R.; Li, Q.; Smith, L. M. Detection of Large Ions in Time-of-Flight Mass Spectrometry: Effects of Ion Mass and Acceleration Voltage on Microchannel Plate Detector Response. *Journal of The American Society for Mass Spectrometry* **2014**, *25*, 1374–1383.

(38) Keldysh, L. V. Ionization in the field of a strong electromagnetic wave. *Soviet Physics JETP* **1965**, *20*, 1307–1314.

(39) Brummel, C.; Willey, K.; Vickerman, J.; Winograd, N. Ion beam induced desorption with postionization using high repetition femtosecond lasers. *International Journal of Mass Spectrometry and Ion Processes* **1995**, *143*, 257–270.

(40) Ledingham, K.; Singhal, R. High intensity laser mass spectrometry–a review. *International Journal of Mass Spectrometry and Ion Processes* **1997**, *163*, 149–168.

(41) Soltwisch, J.; Jaskolla, T. W.; Hillenkamp, F.; Karas, M.; Dreisewerd, K. Ion Yields in UV-MALDI Mass Spectrometry As a Function of Excitation Laser Wavelength and Optical and Physico-Chemical Properties of Classical and Halogen-Substituted MALDI Matrixes. *Analytical Chemistry* **2012**, *84*, 6567–6576.

(42) Robinson, K. N.; Steven, R. T.; Bunch, J. Matrix Optical Absorption in UV-MALDI MS. *Journal of The American Society for Mass Spectrometry* **2018**, *29*, 501–511.

(43) Ingendoha, A.; Karasa, M.; Hillenkamp, F.; Giessmannb, U. Factors affecting the resolution in matrix-assisted mass spectrometry. *International Journal of Mass Spectrometry and Ion Processes* **1994**, *131*, 345–354.

(44) Dreisewerd, K. The Desorption Process in MALDI. *Chemical Reviews* **2003**, *103*, 395–426.

(45) Qiao, H.; Spicer, V.; Ens, W. The effect of laser profile, fluence, and spot size on sensitivity in orthogonal-injection matrix-assisted laser desorption/ionization time-of-flight mass spectrometry. *Rapid Communications in Mass Spectrometry* **2008**, *22*, 2779–2790.

(46) Ahn, S. H.; Park, K. M.; Bae, Y. J.; Kim, M. S. Quantitative reproducibility of mass spectra in matrix-assisted laser desorption ionization and unraveling of the mechanism for gas-phase peptide ion formation. *Journal of Mass Spectrometry* **2013**, *48*, 299–305.

(47) Knochenmuss, R. MALDI ionization mechanisms: the coupled photophysical and chemical dynamics model correctly predicts temperature-selected spectra. *Journal of Mass Spectrometry* **2013**, *48*, 998–1004.

(48) Bae, Y. J.; Kim, M. S. A Thermal Mechanism of Ion Formation in MALDI. *Annual Review of Analytical Chemistry* **2015**, *8*, 41–60.

(49) Wu, K. J.; Shaler, T. A.; Becker, C. H. Time-of-Flight Mass Spectrometry Of Underivatized Single-Stranded DNA Oligomers by Matrix-Assisted Laser Desorption. *Analytical Chemistry* **1994**, *66*, 1637–1645.

(50) Karas, M.; Bahr, U.; Strupat, K.; Hillenkamp, F.; Tsarbopoulos, A.; Pramanik, B. N. Matrix Dependence of Metastable Fragmentation of Glycoproteins in MALDI TOF Mass Spectrometry. *Analytical Chemistry* **1995**, *67*, 675–679.

(51) Christian, N. P.; Colby, S. M.; Giver, L.; Houston, C. T.; Arnold, R. J.; Ellington, A. D.; Reiily, J. P. High resolution matrix-assisted laser desorption/ionization time-of-flight analysis of single-stranded DNA of 27 to 68 nucleotides in length. *Rapid Communications in Mass Spectrometry* **1995**, *9*, 1061–1066.

(52) Kaufmann, R.; Chaurand, P.; Kirsch, D.; Spengler, B. Post-source Decay and Delayed Extraction in Matrix-assisted Laser Desorption/Ionization-Reflectron Time-of-Flight Mass Spectrometry. Are There Trade-offs? *Rapid Communications in Mass Spectrometry* **1996**, *10*, 1199–1208.

(53) Spengler, B.; Kirsch, D.; Kaufmann, R.; Cotter, R. J. Metastable decay of peptides and proteins in matrix-assisted laser-desorption mass spectrometry. *Rapid Communications in Mass Spectrometry* **1991**, *5*, 198–202.

(54) Wang, B. H.; Dreisewerd, K.; Bahr, U.; Karas, M.; Hillenkamp, F. Gas-Phase cationization and protonation of neutrals generated by matrix-assisted laser desorption. *Journal of the American Society for Mass Spectrometry* **1993**, *4*, 393–398.